

Supporting Information

Solvent-etching-induced *in situ* crystal structure transformation in hydrogen-bonded organic frameworks

Xiaokang Wang,^a Hongyan Liu,^a Meng Sun,^a Fei Gao,^a Xueying Feng,^a Mingming Xu,^a Yutong Wang,^{ab} Weidong Fan ^{*a} and Daofeng Sun ^{*a}

^aState Key Laboratory of Heavy Oil Processing, Shandong Key Laboratory of Intelligent Energy Materials, School of Materials Science and Engineering, China University of Petroleum (East China), Qingdao Shandong 266580, China.

^bInorganic Chemistry I, Technische Universität Dresden, Bergstrasse 66, 01069 Dresden, Germany.

*Corresponding author. E-mail: dfsun@upc.edu.cn; wdfan@upc.edu.cn

Table of Contents

| | |
|---|------------|
| Experimental Procedures | S2 |
| Materials and instruments | S2 |
| Synthesis of ligand | S3 |
| Synthesis of UPC-HOFs | S5 |
| Single-crystal X-ray diffraction | S6 |
| Gas sorption measurements | S7 |
| Computational methods | S8 |
| Figures S1-S22 | S9 |
| Tables S1-S2 | S18 |
| References | S20 |

Experimental Procedures

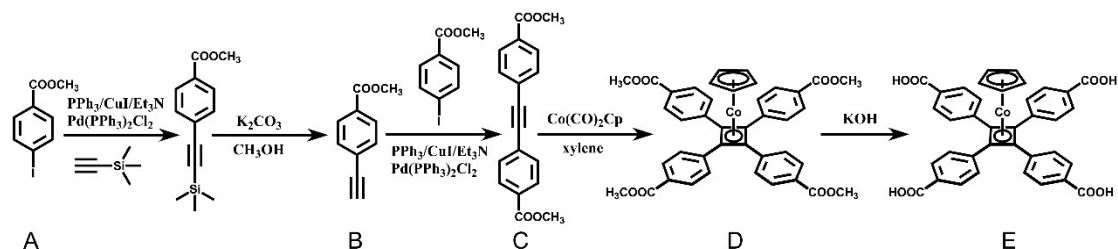
Materials and instruments

All reagents were commercially available and used without further purification.

¹H NMR spectrum was obtained on an Inova 500 MHz spectrometer. Single crystal X-ray diffraction experiments were carried out on a SuperNova diffractometer equipped with mirror Cu-K α radiation ($\lambda = 1.54184 \text{ \AA}$) and an Eos CCD detector. Powder X-ray diffraction (PXRD) was carried out on a Bruker D8-Focus Bragg-Brentano X-ray powder diffractometer equipped with a Cu sealed tube at 40 kV and 15 mA. Infrared (IR) spectroscopy spectrum was collected on a Nicolet 330 FTIR Spectrometer within 4000-400 cm^{-1} region. Gas sorption measurements were conducted on a Micromeritics ASAP 2020 surface area analyzer.

Synthesis of ligand

[Tetrakis(4-carboxyphenyl)cyclobutadiene]cyclopentadienylcobalt (H_4L , E) was synthesized according to previous literature.¹



Scheme S1 Synthetic procedure of ligand: (A) Methyl 4-iodobenzoate, (B) Methyl 4-ethynylbenzoate, (C) Dimethyl 4,4'-(ethyne-1,2-diyl)dibenzoate, (D) [Tetramethyl 4,4',4'',4'''-(cyclobuta-1,3-diene-1,2,3,4-tetrayl)tetrabenzoate]cyclopentadienylcobalt, and (E) [Tetrakis(4-carboxyphenyl)cyclobutadiene]cyclopentadienylcobalt.

Methyl 4-ethynylbenzoate (B)

The mixture of A (3.93 g, 15 mmol), $Pd(PPh_3)_2Cl_2$ (0.57 g, 0.75 mmol), PPh_3 (0.39 g, 1.5 mmol) and CuI (0.17 g, 0.9 mmol) in freshly distilled Et_3N (30 mL) was added dropwise a solution of (trimethylsilyl)acetylene (4.2 mL, 30 mmol) in Et_3N (5 mL) at 90 °C under nitrogen atmosphere for 24 h. After 100 mL ethyl acetate was added, the mixture was filtered and the solvent was removed under reduced pressure. Then methanol (30 mL) and K_2CO_3 (3 g) were added at room temperature for 3 h. Upon completion, methanol was removed under reduced pressure, and water was added to the residue, which was extracted with CH_2Cl_2 . The organic phase was washed with saturated salt water and finally dried over $MgSO_4$. The CH_2Cl_2 was removed under reduced pressure and a purification by column chromatography on silica gel (petroleum ether/ethyl acetate = 10/1). 1H NMR ($CDCl_3$): δ = 7.54 (d, 2H), 7.99 (d, 2H), 3.92 (s, 3H), 3.23 (s, 1H).

Dimethyl 4,4'-(ethyne-1,2-diyl)dibenzoate (C)

The mixture of A (3.93 g, 15 mmol), B (2.4 g, 15 mmol), $Pd(PPh_3)_2Cl_2$ (0.38 g, 0.54 mmol), CuI (0.2 g, 1.12 mmol) and PPh_3 (0.296 g, 1.12 mmol) was put into a 250 mL flask. The flask was degassed and refilled with nitrogen, which was repeated for three times. Degassed Et_3N (100 mL) was added. The mixture was stirred under reflux for 2 d. The solvent was removed and the residual power was suspended in CH_2Cl_2/H_2O and

filtered. The organic phase was dried with MgSO₄. After the solvent was removed, the residue was purified by column chromatography (CH₂Cl₂ or CHCl₃). ¹H NMR (CDCl₃): δ = 3.87 (s, 6H), 7.53 (d, 4H), 7.96 (d, 4H).

[Tetramethyl 4,4',4'',4'''-(cyclobuta-1,3-diene-1,2,3,4-tetrayl)tetrabenzoate]cyclopentadienylcobalt (D)

C (4.2 g, 13 mmol) was charged into a 500 mL two-necked Schlenk flask. The flask was transferred into the glove box and Co(CO)₂Cp (1.1 g, 6.5 mmol) was added. After the flask was removed out of the box, 400 mL degassed xylene was added through a canula. The mixture was heated to reflux under N₂ for 20 ~ 24 h. A lot of precipitates formed when the mixture was cooled in an ice bath. The solid was collected by filtration and washed with hexanes several times. The crude was purified by column chromatography with CHCl₃ as the eluent to give pure product. ¹H NMR (CDCl₃): δ = 1.26 (s, 12H), 3.93 (s, 12H), 4.65 (s, 5H), 7.45 (d, 8H), 7.89 (d, 8H).

[Tetrakis(4-carboxyphenyl)cyclobutadiene]cyclopentadienylcobalt (E)

D was suspended in 100 mL THF, to which was added 20 mL 2 M KOH aqueous solution. The mixture was refluxed overnight. THF was removed on rotary evaporator and diluted hydrochloric acid was added into the aqueous solution until the solution became acidic. The solid was collected by filtration, washed with water several times and dried in the air. ¹H NMR (*d*₆-DMSO): δ = 4.77 (s, 5H), 7.47 (d, 8H), 7.84 (d, 8H), 12.86 (s, 4H).

Synthesis of UPC-HOFs

H₄L precursor (10 mg) was added to a glass vial (10 mL) with 1 mL *N,N'*-dimethylformamide (DMF) and 3 mL dichloromethane. After slow evaporation of solvents for 2 weeks, yellow block crystal of UPC-HOF-12 was obtained. UPC-HOF-13 was prepared by exposing UPC-HOF-12 to DMF vapor for a week.

Single-crystal X-ray diffraction

The as-synthesized crystal of UPC-HOF-12 was taken from the mother liquid without further treatment, transferred to oil and mounted on to a loop for single crystal X-ray data collection. The crystal data of UPC-HOF-12 was collected on an Agilent Technologies SuperNova diffractometer equipped with graphite monochromatic Cu K α radiation ($\lambda = 1.54184 \text{ \AA}$). With the help of Olex2, the structure of UPC-HOF-12 was solved with the Superflip structure solution program using charge flipping and refined with the ShelXL refinement package using least squares minimization. The structure of UPC-HOF-12 was treated anisotropically, whereas the hydrogen atoms were placed in calculated ideal positions and refined as riding on their respective nonhydrogen atoms. PLATON and SQUEEZE² were used to calculate the diffraction contribution of the solvent molecules in UPC-HOF-12 and thereby produced a set of partly solvent-free diffraction intensities.

The as-synthesized crystal of UPC-HOF-13 was transferred to oil and mounted on to a loop for single crystal X-ray data collection. The crystal data of UPC-HOF-13 was collected on an Agilent Technologies SuperNova diffractometer equipped with graphite monochromatic Cu K α radiation ($\lambda = 1.54184 \text{ \AA}$). With the help of Olex2, the structure of UPC-HOF-13 was solved with the Superflip structure solution program using charge flipping and refined with the ShelXL refinement package using least squares minimization. The structure of UPC-HOF-13 was treated anisotropically, whereas the hydrogen atoms were placed in calculated ideal positions and refined as riding on their respective nonhydrogen atoms. No SQUEEZE was run on UPC-HOF-13.

The crystal data of UPC-HOF-12 and UPC-HOF-13 have been deposited to Cambridge Crystallographic Data Center (CCDC) as 2376496 and 2376497, respectively.

Gas sorption measurements

The activated samples were prepared by immersing the as-synthesized UPC-HOF-12 and UPC-HOF-13 in deionized water for solvent exchange followed by activation at 373 K under vacuum for 10 h. Gas adsorption experiments containing N₂ at 77 K, CO₂ at 195 K, and C₂H₂, CO₂, and CH₄ at 273 and 298 K, were performed by using ASAP-2020 surface area analyzer. Liquid nitrogen bath and dry ice-acetone bath was used to stabilize the temperature at 77 and 195 K, respectively, whereas other test temperatures were maintained via a circulating water bath.

Computational methods

Isosteric heat of adsorption

A Virial equation comprising the temperature-independent parameters a_i and b_j was employed to calculate the enthalpies of adsorption for C₂H₂ and CO₂ in UPC-HOF-13, which were measured at 273 and 298 K.

$$\ln P = \ln N + \frac{1}{T} \sum_i^m a_i N_i + \sum_j^n b_j N_j$$

$$Q_{st} = -R \sum_{i=0}^m a_i N_i$$

Here, P is the pressure expressed in mmHg, N is the amount adsorbed in mmol/g, T is the temperature in K, a_i and b_j are virial coefficients, and m , n represent the number of coefficients required to adequately describe the isotherms (herein, $m=5$ and $n=2$). Q_{st} is the coverage-dependent isosteric heat of adsorption and R is the universal gas constant.

Selectivity based on ideal adsorbed solution theory

Before estimating the selectivity for binary gas mixture, the single-component gas adsorption isotherms were first fitted to a dual-site Langmuir-Freundlich (DSLFL) model:

$$q = q_{A,sat} \frac{b_A p^{n_1}}{1 + b_A p^{n_1}} + q_{B,sat} \frac{b_B p^{n_2}}{1 + b_B p^{n_2}}$$

where q is the amount of adsorbed gas (mmol/g), p is the bulk gas phase pressure (kPa), q_{sat} is the saturation amount (mmol/g), b is the Langmuir-Freundlich parameter (kPa⁻¹), and n is the Langmuir-Freundlich exponent (dimensionless) for two adsorption sites A and B indicating the presence of weak and strong adsorption sites. b_A and b_B are both temperature-dependent.

$$b_A = b_{A0} \exp\left(\frac{E_A}{RT}\right); b_B = b_{B0} \exp\left(\frac{E_B}{RT}\right)$$

The adsorption selectivity S_{ads} was calculated by ideal adsorbed solution theory:

$$S_{ads} = \frac{q_1/q_2}{p_1/p_2}$$

where q_1 and q_2 are the molar loadings in the adsorbed phase in equilibrium with the bulk gas phase, p_1 and p_2 are partial pressure.

Figures S1-S22

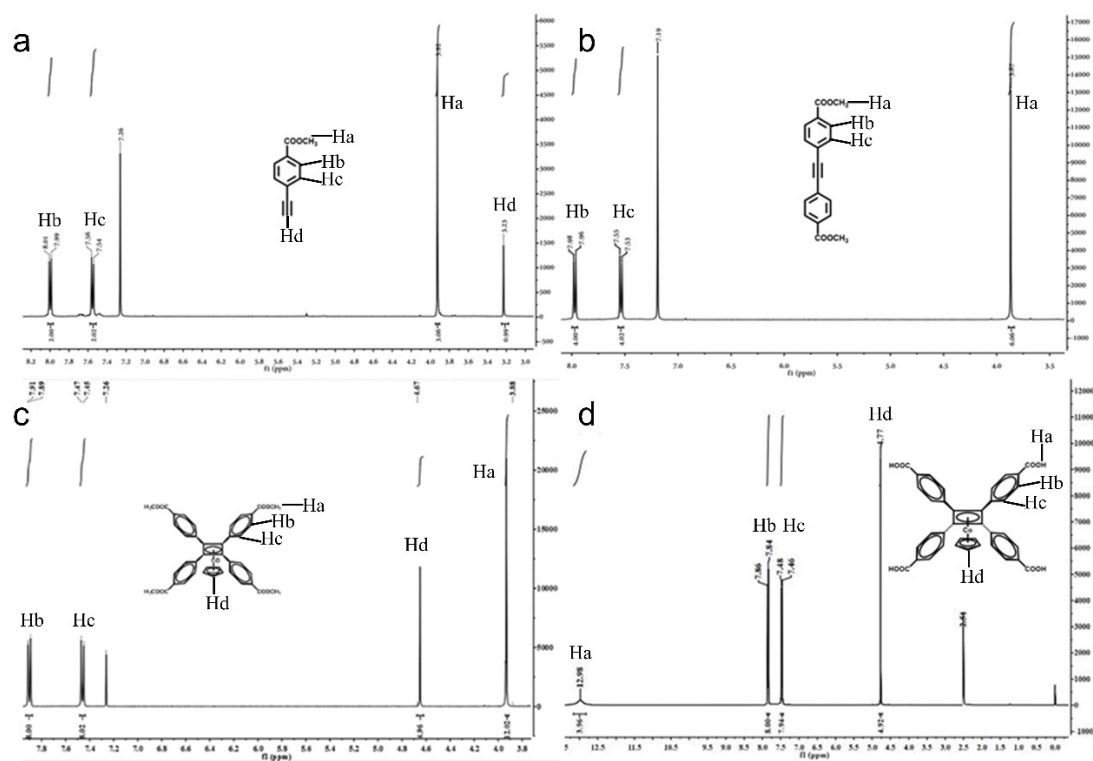


Fig. S1 ^1H NMR spectrum of synthesized products: (a) Methyl 4-ethynylbenzoate, (b) Dimethyl 4,4'-(ethyne-1,2-diyl)dibenzoate, (c) [Tetramethyl 4,4',4'',4'''-(cyclobuta-1,3-diene-1,2,3,4-tetrayl)tetrabenzoate]cyclopentadienylcobalt, and (d) [Tetrakis(4-carboxyphenyl)cyclobutadiene]cyclopentadienylcobalt.

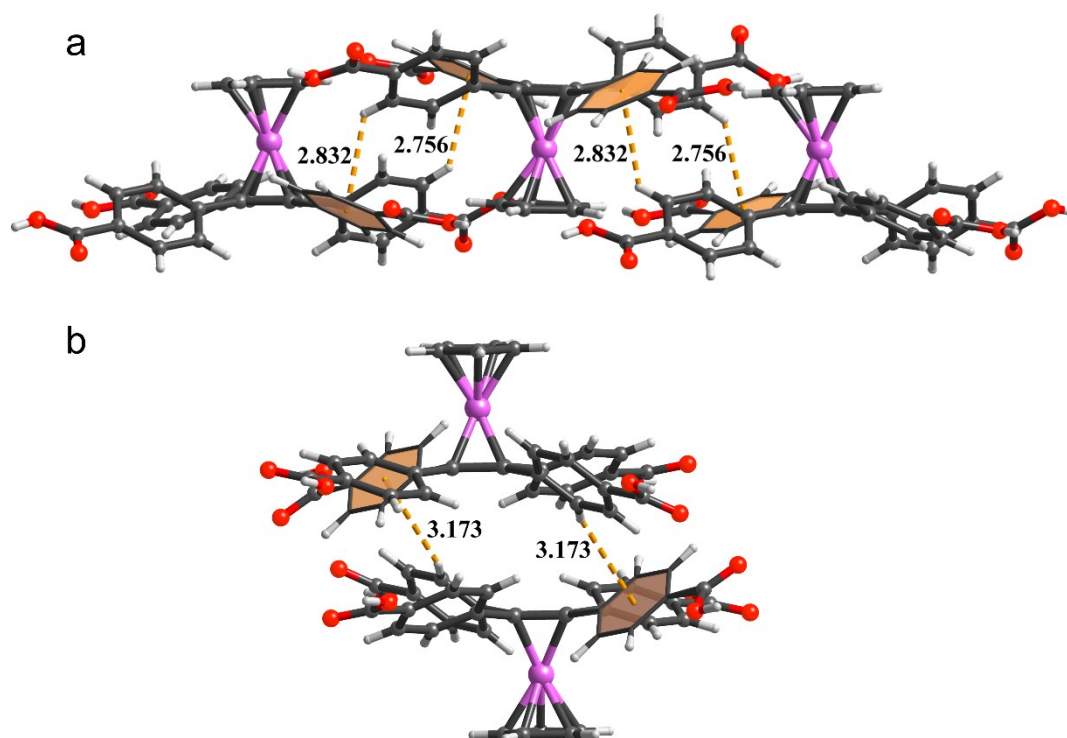


Fig. S2 (a) Intralayer $\text{C-H}\cdots\pi$ interactions and (b) interlayer $\text{C-H}\cdots\pi$ interactions in UPC-HOF-12. Distances are given in Å.

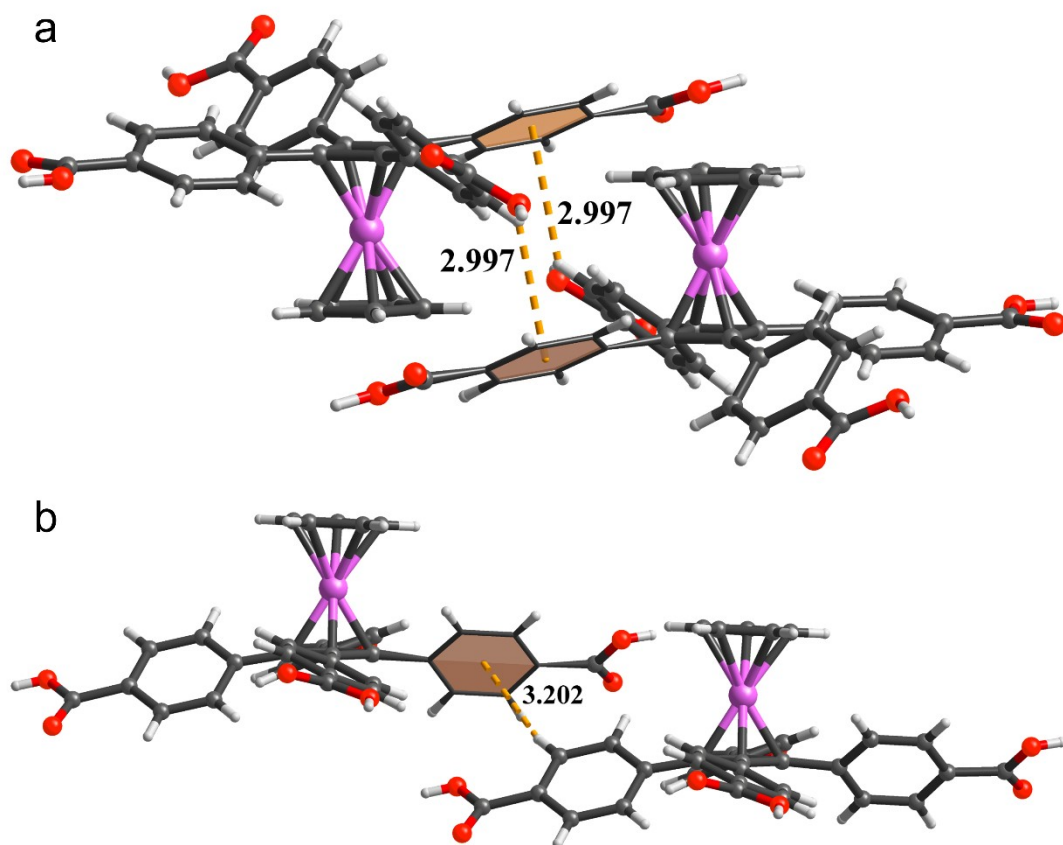


Fig. S3 (a) Intralayer C–H... π interactions and (b) interlayer C–H... π interactions in UPC-HOF-13. Distances are given in Å.

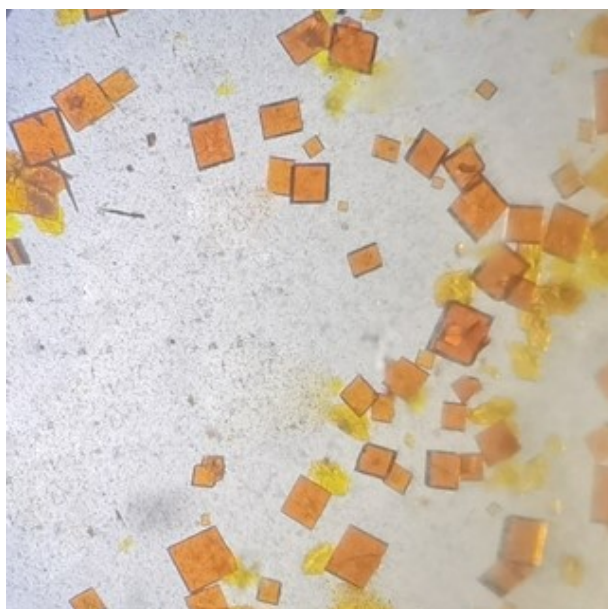


Fig. S4 Optical photograph of UPC-HOF-12.

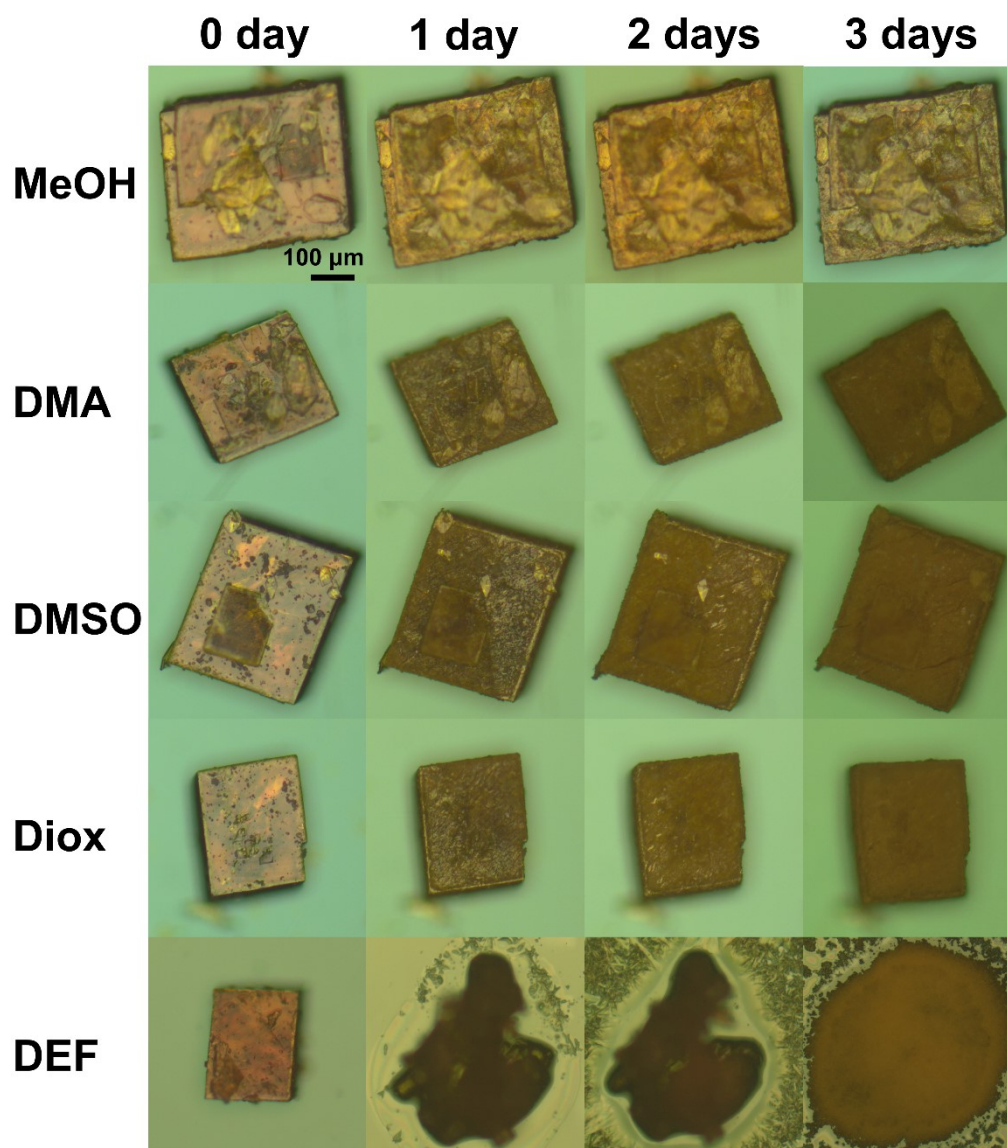


Fig. S5 Optical photographs of UPC-HOF-12 exposed to vapors of different organic solvents. MeOH= methanol, DMA = *N,N'*-dimethylacetamide, DMSO = dimethyl sulfoxide, Diox = 1,4-dioxane, DEF = *N,N'*-diethylformamide.

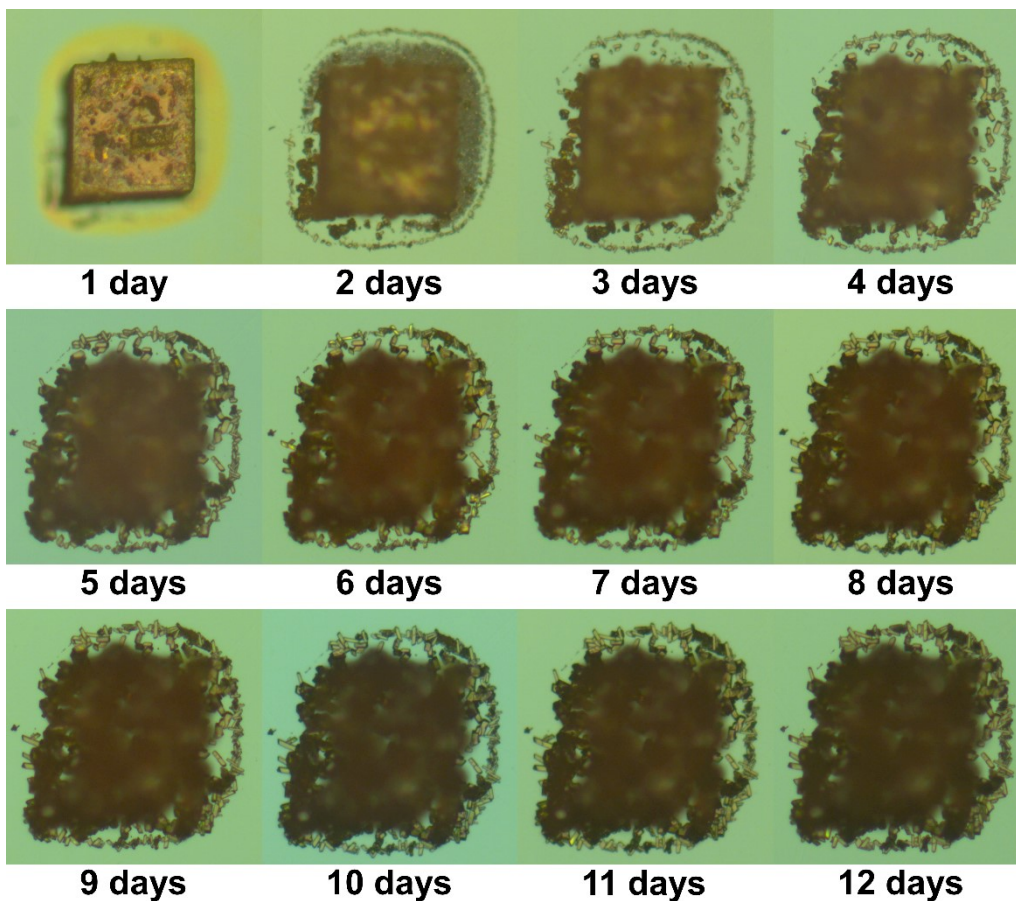


Fig. S6 Optical photographs of UPC-HOF-12 exposed to DMF vapor for different times.

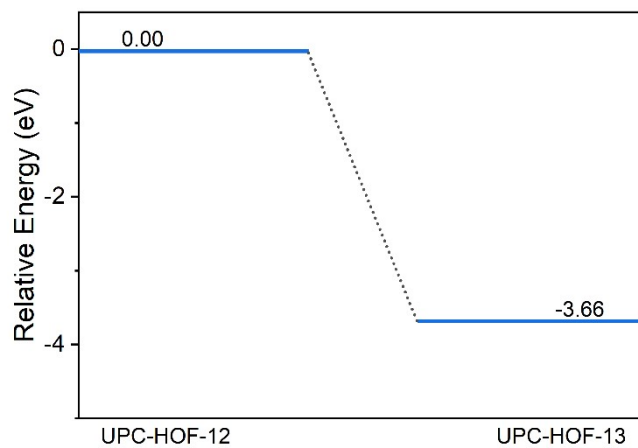


Fig. S7 DFT-calculated relative energy of UPC-HOF-12 and UPC-HOF-13.

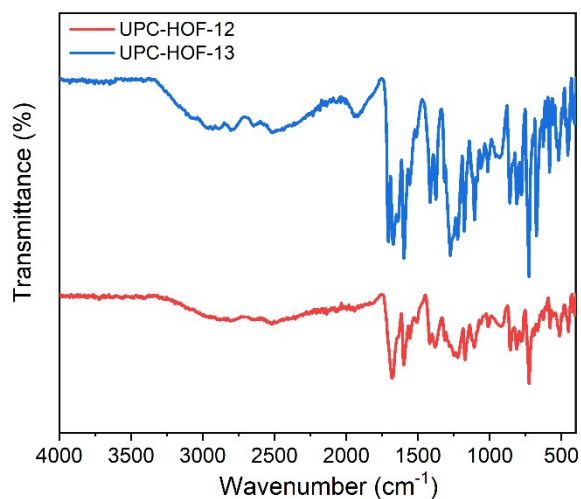


Fig. S8 Infrared spectra of UPC-HOF-12 and UPC-HOF-13.

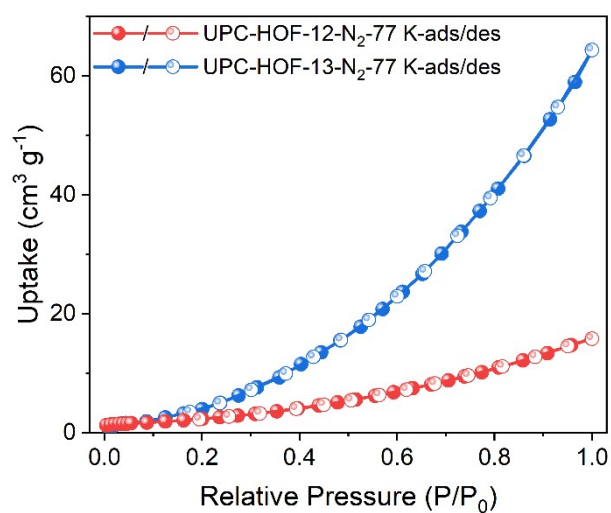


Fig. S9 N₂ adsorption/desorption isotherms of UPC-HOF-12 and UPC-HOF-13 at 77 K.

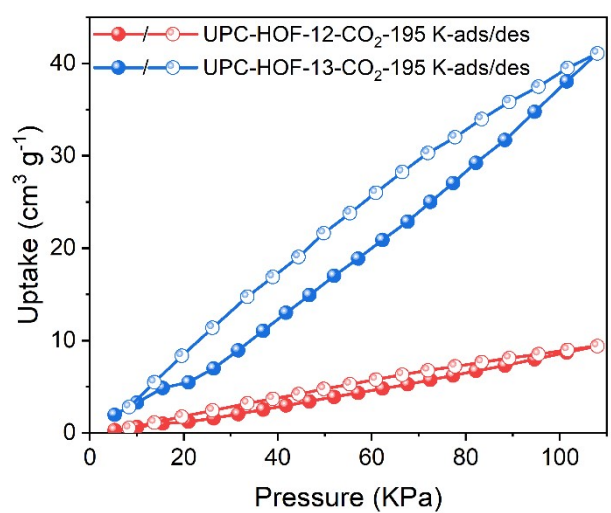


Fig. S10 CO₂ adsorption/desorption isotherms of UPC-HOF-12 and UPC-HOF-13 at 195 K.

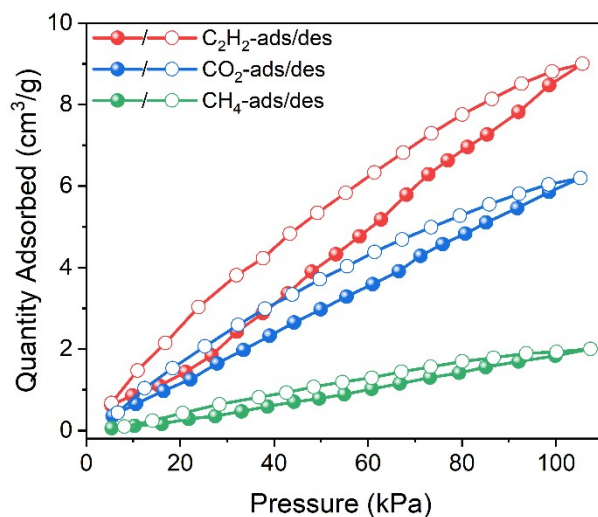


Fig. S11 Single-component C_2H_2 , CO_2 , and CH_4 adsorption/desorption isotherms of UPC-HOF-12 at 273 K.

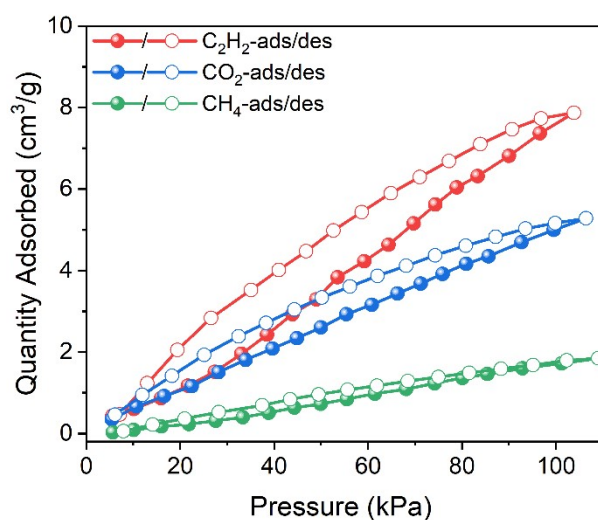


Fig. S12 Single-component C_2H_2 , CO_2 , and CH_4 adsorption/desorption isotherms of UPC-HOF-12 at 298 K.

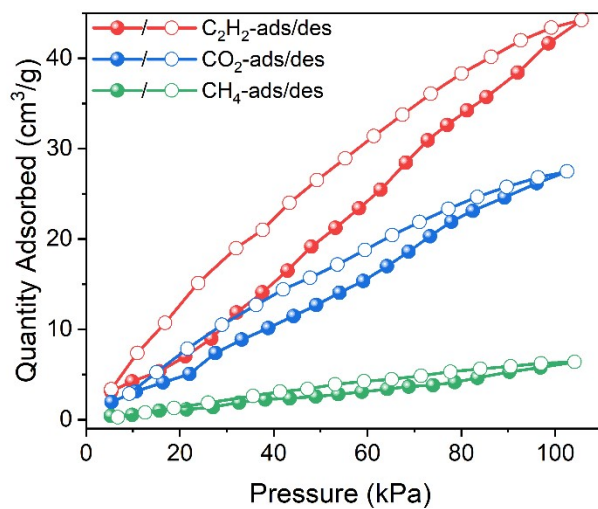


Fig. S13 Single-component C_2H_2 , CO_2 , and CH_4 adsorption/desorption isotherms of UPC-HOF-13 at 273 K.

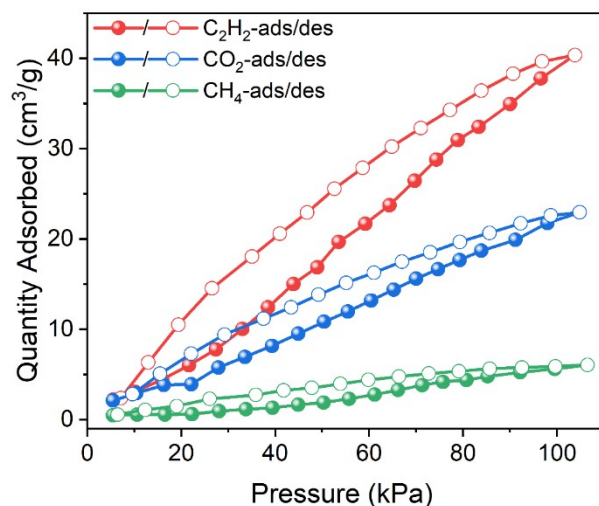


Fig. S14 Single-component C_2H_2 , CO_2 , and CH_4 adsorption/desorption isotherms of UPC-HOF-13 at 298 K.

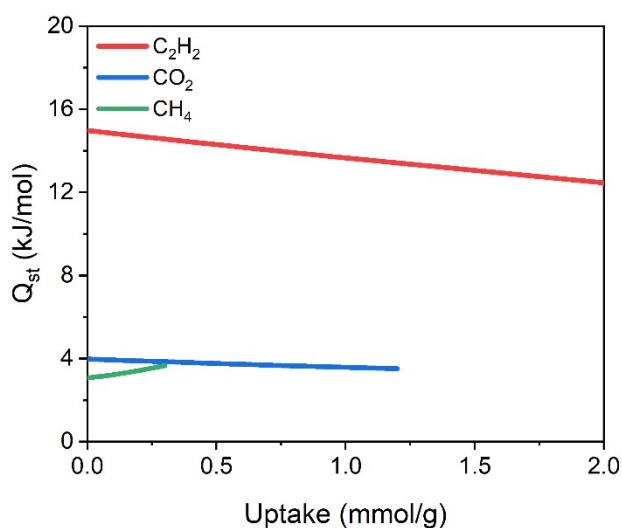


Fig. S15 Adsorption enthalpy of UPC-HOF-13 for C_2H_2 , CO_2 , and CH_4 .

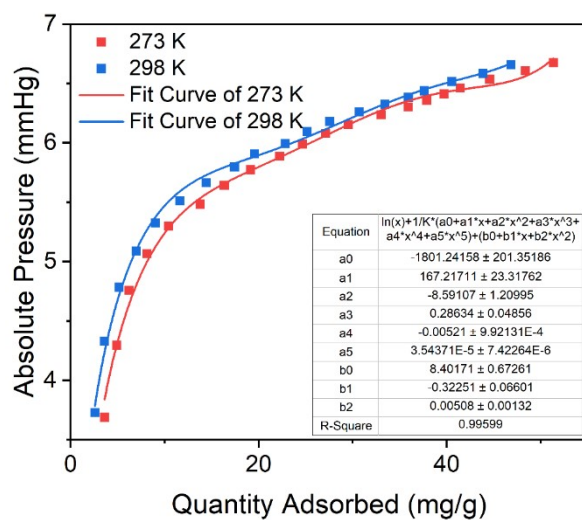


Fig. S16 Virial fitting of C_2H_2 for UPC-HOF-13.

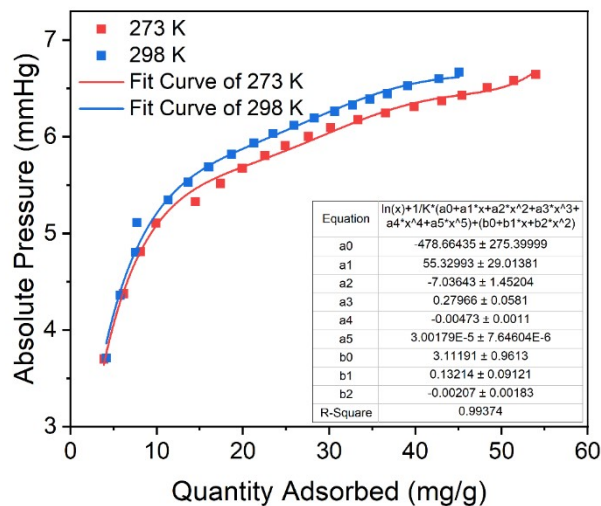


Fig. S17 Virial fitting of CO₂ for UPC-HOF-13.

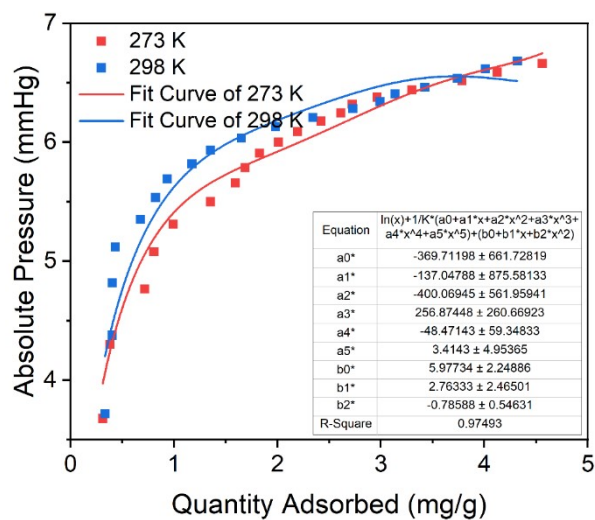


Fig. S18 Virial fitting of CH₄ for UPC-HOF-13.

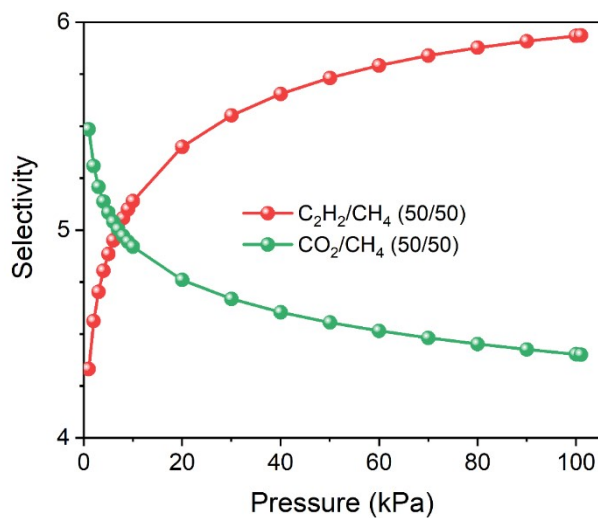


Fig. S19 IAST selectivity of UPC-HOF-13 for C₂H₂/CH₄ and CO₂/CH₄ at 273 K.

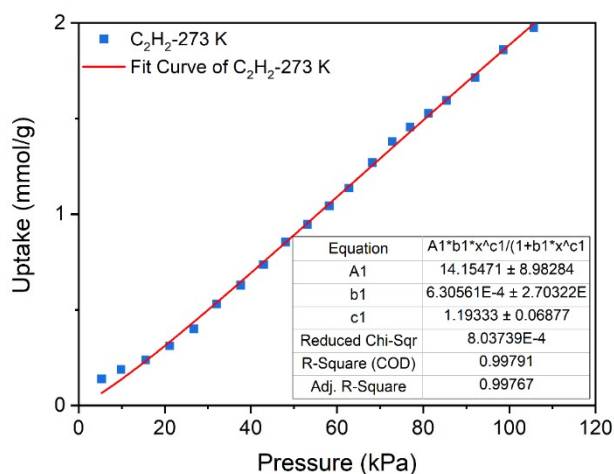


Fig. S20 Langmuir-Freundlich fitting of C_2H_2 for UPC-HOF-13 at 273 K.

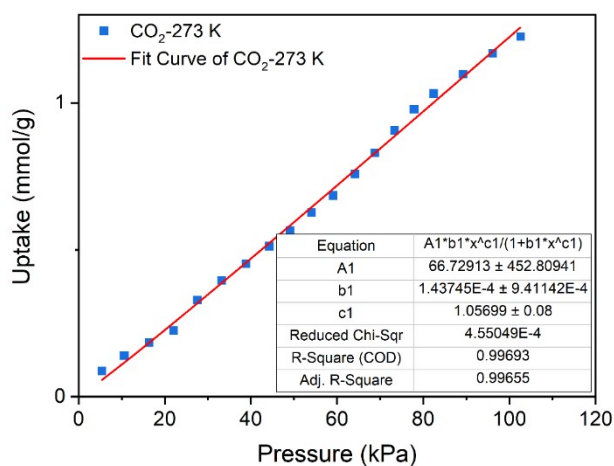


Fig. S21 Langmuir-Freundlich fitting of CO_2 for UPC-HOF-13 at 273 K.

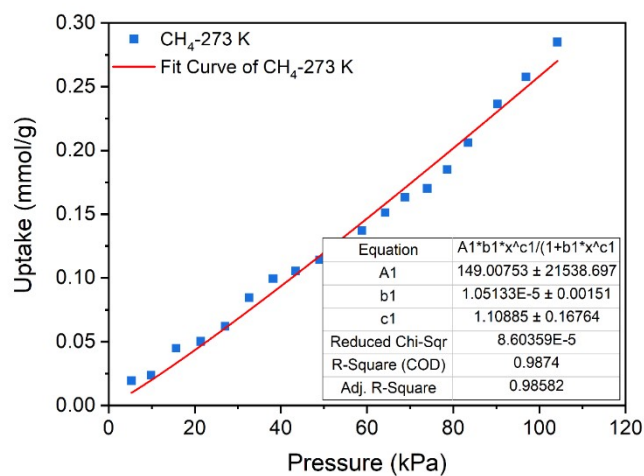


Fig. S22 Langmuir-Freundlich fitting of CH_4 for UPC-HOF-13 at 273 K.

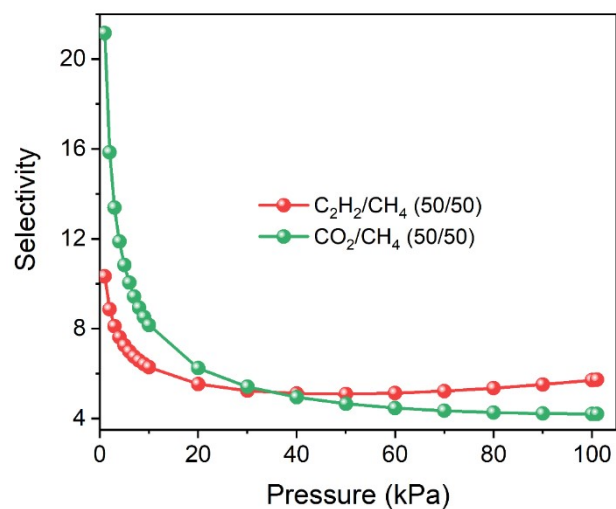


Fig. S23 IAST selectivity of UPC-HOF-13 for C_2H_2/CH_4 and CO_2/CH_4 at 298 K.

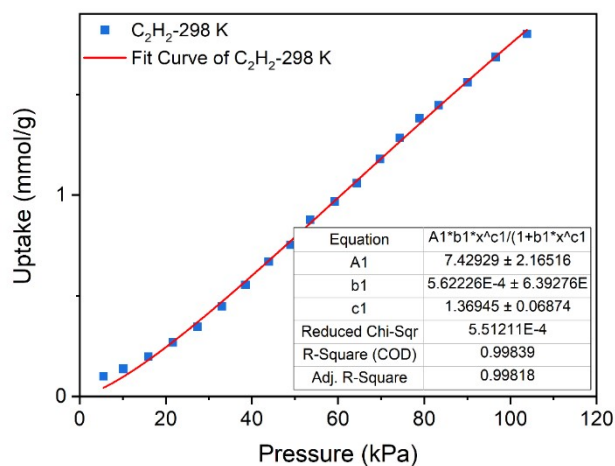


Fig. S24 Langmuir-Freundlich fitting of C_2H_2 for UPC-HOF-13 at 298 K.

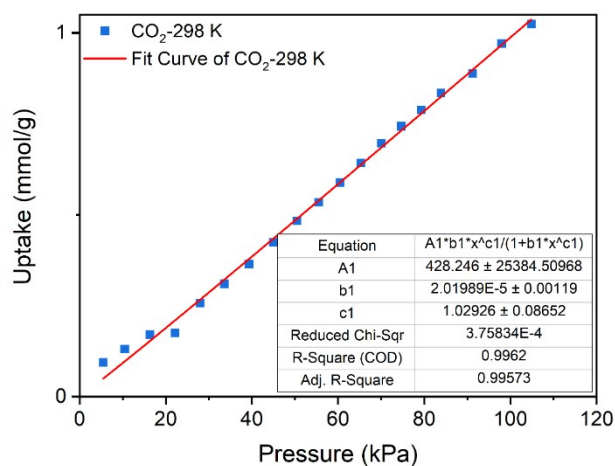


Fig. S25 Langmuir-Freundlich fitting of CO_2 for UPC-HOF-13 at 298 K.

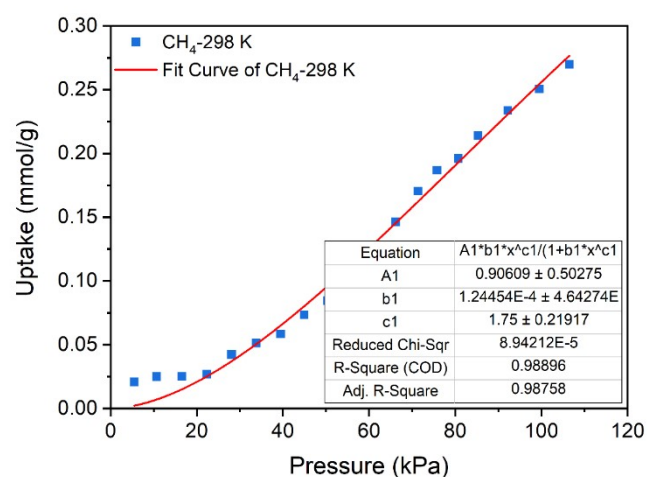


Fig. S26 Langmuir-Freundlich fitting of CH₄ for UPC-HOF-13 at 298 K.

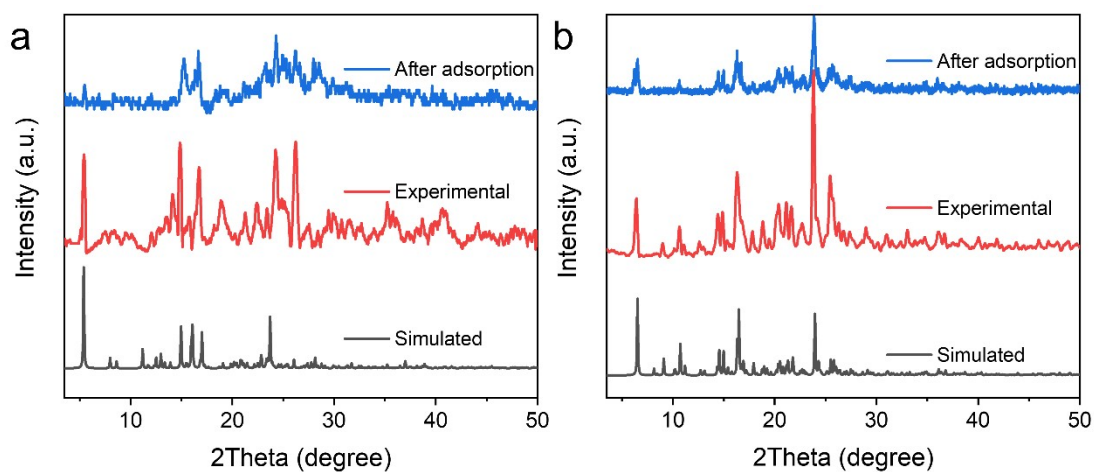


Fig. S27 PXRD patterns of (a) UPC-HOF-12 and (b) UPC-HOF-13.

Tables S1-S2

Table S1. Crystal data of UPC-HOFs.

| Compound | UPC-HOF-12 | UPC-HOF-13 |
|---|--|--|
| CCDC | 2376496 | 2376497 |
| Formula | C ₄₃ H ₃₉ CoN ₂ O ₁₀ | C ₄₃ H ₃₉ CoN ₂ O ₁₀ |
| Formula weight | 802.69 | 802.69 |
| Temperature/K | 296.12(10) | 294.2(3) |
| Crystal system | monoclinic | triclinic |
| Space group | <i>P2₁/c</i> | <i>P-1</i> |
| a/Å | 17.7931(4) | 11.4687(5) |
| b/Å | 14.9960(3) | 13.0070(6) |
| c/Å | 16.0649(3) | 14.1101(5) |
| α/° | 90 | 74.105(4) |
| β/° | 113.130(3) | 88.003(3) |
| γ/° | 90 | 71.393 (4) |
| Volume/Å ³ | 3941.94(16) | 1915.37(15) |
| Z | 4 | 2 |
| ρ g/cm ³ | 1.353 | 1.392 |
| μ/mm ⁻¹ | 3.925 | 4.039 |
| F(000) | 1672.0 | 836.0 |
| 2θ range for data collection | 7.998-141.488 | 7.464-141.152 |
| | -21 ≤ h ≤ 21 | -14 ≤ h ≤ 13 |
| Index ranges | -16 ≤ k ≤ 18 | -15 ≤ k ≤ 15 |
| | -13 ≤ l ≤ 19 | -17 ≤ l ≤ 7 |
| Reflections collected | 15488 | 14237 |
| R _{int} | 0.0345 | 0.0276 |
| Data/restraints/parameters | 7411/30/513 | 7199/0/516 |
| Goodness-of-fit on F ² | 1.029 | 1.038 |
| Final R indexes [I ≥ 2σ (I)] | R ₁ = 0.0662 wR ₂ = 0.1754 | R ₁ = 0.0439 wR ₂ = 0.1083 |
| Final R indexes [all data] | R ₁ = 0.0889 wR ₂ = 0.1995 | R ₁ = 0.0577 wR ₂ = 0.1160 |
| Largest diff. peak/hole /eÅ ⁻³ | 1.08/-0.47 | 0.37/-0.28 |

Table S2. Details of hydrogen-bonding in UPC-HOF-12.

| D-H...A | D-H (Å) | H...A (Å) | D...A (Å) | D-H...A (°) | symop-for-A |
|-------------|---------|-----------|-----------|-------------|---------------|
| O2-H2...O9 | 0.82 | 1.98 | 2.757(4) | 157 | 1+x, y, 1+z |
| O4-H4...O9 | 0.82 | 1.85 | 2.660(5) | 171 | 1+x, y, z |
| O5-H5...O10 | 0.82 | 1.86 | 2.677(5) | 171 | -1+x, y, z |
| O8-H8...O10 | 0.82 | 1.92 | 2.706(4) | 162 | -1+x, y, -1+z |

Table S3. Details of hydrogen-bonding in UPC-HOF-13.

| D-H...A | D-H (Å) | H...A (Å) | D...A (Å) | D-H...A (°) | symop-for-A |
|-------------|---------|-----------|-----------|-------------|----------------|
| O2-H2...O10 | 0.82 | 1.79 | 2.606(4) | 175 | 1+x, y, z |
| O4-H4...O3 | 0.96(7) | 1.71(7) | 2.671(3) | 179(10) | 1-x, -y, -z |
| O6-H6...O7 | 0.82 | 1.96 | 2.773(3) | 174 | -1-x, 1-y, 1-z |
| O8-H8...O9 | 0.82 | 1.74 | 2.557(3) | 174 | -x, 1-y, 2-z |

Table S4. Comparison of adsorption performance in HOFs at room temperature.

| Materials | Q_{st} (kJ/mol) | | | IAST selectivity | | Ref. |
|------------|-------------------------------|-----------------|-----------------|--|----------------------------------|-----------|
| | C ₂ H ₂ | CO ₂ | CH ₄ | C ₂ H ₂ /CH ₄ | CO ₂ /CH ₄ | |
| UPC-HOF-13 | 14.9 | 3.9 | 3.0 | 5.7 | 4.2 | This work |
| HOF-5a | 27.6 | 22.8 | 19.2 | 13.6 ^a | 5.0 ^a | 3 |
| HOF-9a | – | 23.5 | 14.4 | – | 2.9 ^a | 4 |
| HOF-11a | 18.8 | 19.6 | 16.6 | 7.2 | 3.4 | 5 |
| HOF-12 | – | 28.5 | – | – | 5.3 | 6 |
| HOF-14 | – | – | – | 3.7 | – | 7 |
| HOF-16a | 23.0 | 21.6 | 18.5 | 107 | 8.9 | 5 |
| JLU-SOF1-R | – | 34.3 | 18.9 | – | 3.9 | 8 |
| BTBA-1a | – | 25.1 | – | – | 14 | 9 |
| PTBA-1a | – | 33.7 | – | – | 6 | 9 |
| HOF-BTB | 24.3 | – | – | 9.3 ^b | – | 10 |
| SOF-1a | 36.2 | 27.6 | 20.8 | – | 4.2 | 11 |
| SOF-7a | – | 21.6 | – | – | 9.1 | 12 |

^a 296 K, ^b 295 K

References

- (1) Wang, Y.; Hao, C.; Fan, W.; Fu, M.; Wang, X.; Wang, Z.; Zhu, L.; Li, Y.; Lu, X.; Dai, F.; et al. One-step Ethylene Purification from an Acetylene/Ethylene/Ethane Ternary Mixture by Cyclopentadiene Cobalt-Functionalized Metal-Organic Frameworks. *Angew. Chem., Int. Ed.* **2021**, *60* (20), 11350–11358. DOI: 10.1002/anie.202100782.
- (2) Spek, A. L. PLATONSQUEEZE: a tool for the calculation of the disordered solvent contribution to the calculated structure factors. *Acta Cryst. C* **2015**, *71* (1), 9-18. DOI: 10.1107/s2053229614024929.
- (3) Wang, H.; Li, B.; Wu, H.; Hu, T.-L.; Yao, Z.; Zhou, W.; Xiang, S.; Chen, B. A Flexible Microporous Hydrogen-Bonded Organic Framework for Gas Sorption and Separation. *J. Am. Chem. Soc.* **2015**, *137* (31), 9963–9970. DOI: 10.1021/jacs.5b05644.
- (4) Wang, H.; Wu, H.; Kan, J.; Chang, G.; Yao, Z.; Li, B.; Zhou, W.; Xiang, S.; Cong-Gui Zhao, J.; Chen, B. A Microporous Hydrogen-Bonded Organic Framework with Amine Sites for Selective Recognition of Small Molecules. *J. Mater. Chem. A* **2017**, *5* (18), 8292–8296. DOI: 10.1039/c7ta01364g.
- (5) Cai, Y.; Chen, H.; Liu, P.; Chen, J.; Xu, H.; Alshahrani, T.; Li, L.; Chen, B.; Gao, J. Robust Microporous Hydrogen-Bonded Organic Framework for Highly Selective Purification of Methane from Natural Gas. *Microp. Mesop. Mater.* **2023**, *352*, 112495. DOI: 10.1016/j.micromeso.2023.112495.
- (6) Yang, W.; Zhou, W.; Chen, B. A Flexible Microporous Hydrogen-Bonded Organic Framework. *Cryst. Growth Des.* **2019**, *19* (9), 5184–5188. DOI: 10.1021/acs.cgd.9b00582.
- (7) Wang, B.; Lv, X.-L.; Lv, J.; Ma, L.; Lin, R.-B.; Cui, H.; Zhang, J.; Zhang, Z.; Xiang, S.; Chen, B. A Novel Mesoporous Hydrogen-Bonded Organic Framework with High Porosity and Stability. *Chem. Commun.* **2020**, *56* (1), 66–69. DOI: 10.1039/c9cc07802a.
- (8) Zhou, Y.; Liu, B.; Sun, X.; Li, J.; Li, G.; Huo, Q.; Liu, Y. Self-assembly of Homochiral Porous Supramolecular Organic Frameworks with Significant CO₂ Capture and CO₂/N₂ Selectivities. *Cryst. Growth Des.* **2017**, *17* (12), 6653–6659. DOI: 10.1021/acs.cgd.7b01282.
- (9) Ding, X.; Liu, Z.; Zhang, Y.; Ye, G.; Jia, J.; Chen, J. Binary Solvent Regulated Architecture of Ultra-Microporous Hydrogen-Bonded Organic Frameworks with Tunable Polarization for Highly-Selective Gas Separation. *Angew. Chem. Int. Ed.* **2022**, *61* (13), e202116483. DOI: 10.1002/anie.202116483.
- (10) Yoon, T.-U.; Baek, S. B.; Kim, D.; Kim, E.-J.; Lee, W.-G.; Singh, B. K.; Lah, M. S.; Bae, Y.-S.; Kim, K. S. Efficient Separation of C₂ Hydrocarbons in a Permanently Porous Hydrogen-Bonded Organic Framework. *Chem. Commun.* **2018**, *54* (67), 9360–9363. DOI: 10.1039/c8cc04139c.
- (11) Yang, W.; Greenaway, A.; Lin, X.; Matsuda, R.; Blake, A. J.; Wilson, C.; Lewis, W.; Hubberstey, P.; Kitagawa, S.; Champness, N. R.; et al. Exceptional Thermal Stability in a Supramolecular Organic Framework: Porosity and Gas Storage. *J. Am. Chem. Soc.* **2010**, *132* (41), 14457–14469. DOI: 10.1021/ja1042935.
- (12) Lü, J.; Perez-Krap, C.; Suyetin, M.; Alsmail, N. H.; Yan, Y.; Yang, S.; Lewis, W.; Bichoutskaia, E.; Tang, C. C.; Blake, A. J.; et al. A Robust Binary Supramolecular Organic Framework (SOF) with High CO₂ Adsorption and Selectivity. *J. Am. Chem. Soc.* **2014**, *136* (37), 12828–12831. DOI: 10.1021/ja506577g.